Multifunctional Structural Supercapacitor based on Nitrogen Doped Graphene Nanoflakes Directly Grown on Carbon Fibre Electrodes

Abhijit Ganguly, Anastasios Karakassides, and Pagona Papakonstantinou*

School of Engineering, Engineering Research Institute, Ulster University, Newtownabbey BT37 0QB, United Kingdom

*Corresponding author, e mail address: p.papakonstantinou@ulster.ac.uk

Introduction- Motivation

There is a strong need in electric-based transportation for structural energy storage systems that are lightweight and simultaneously offer both load bearing and energy storage capabilities in a single multifunctional platform. At the forefront of emerging Multifunctional Structural Supercapacitors (**MSS**) technologies are carbon fibre reinforced composites (**CFRP**), promising considerable mass and volume savings over traditional supercapacitors [1]. Current development of MSS [2,3] is mainly based on the assembly of two electrodes made of carbon fiber (**CF**) fabrics separated by single/double dielectric glass fiber (**GF**) fabric separator, infused in a multifunctional solid polymer electrolyte (**SPE**) matrix. However, the commercially available pristine CF electrodes although offer excellent mechanical properties suffer from poor electrochemical storage performance, as they exhibit a surface area that is near 10000 lower than state-of-the art nanomaterials for conventional supercapacitors.

To tackle this deficiency, we modified CF with directly grown graphene nanoflakes (GNFs), 3-dimensional networks of vertically oriented multiple graphene layers [4], to enhance their degree of graphitization and active surface area. Recently, we demonstrated that GNFs directly grown on CF, by microwave plasma enhanced chemical vapour deposition (MW-PECVD), not only improved the interfacial shear strength by 101.5% but simultaneously led to a remarkable 28% enhancement in the tensile strength of the single-fibre [5]. In unison, GNFs-coverage also increased electrical conductivity (60.5% for yarns and 16% for single-fibre) and electrochemical capacitance (by 157% for yarns) in conventional liquid electrolytes [5].

Summary of work performed

In this work, we investigated the electrochemical and mechanical performance of MSS based on GNFs, directly grown on carbon fabric (***CF***) electrodes, infused in a mixture of PEGDGE polymer matrix and ionic liquid (EMITFSI) electrolyte.

Direct growth of GNFs on CF (***gCF***) by rf-PECVD method demonstrated to a significant enhancement of the specific capacitance (C_{sp}) and capacitive energy density (Γ_M), compared to the conventional (control) MSS device consisting of bare CF electrodes a 7.5 times improvement in.

In a second phase of project, we show that activation of GNF-coated fabrics (***UgCF***) by a novel method in a concentrated urea solution introduced a 3.5 at.% nitrogen doping to the hybrid fabrics, which led to another significant leap in C_{sp} and Γ_M, over the control bare CF MSS device.

It was established that the urea activated GNF/CF hierarchical based MSS displayed improvements in the electrochemical performance due to the combined effects of (i) increased graphitized surface area promoting ion accumulation, (ii) high conductivity induced by nitrogen doping, favoring electron transfer efficiency, and (iii) good electrical contact to the CF induced by the direct growth of GNFs.

Overall, in terms of Young's modulus (***E***), the nitrogen doped GNF-based MSS device also offered an retention of structural efficiency of 0.9, showing potential for the "multifunctional" applications.

These findings provide important knowledge for the design of next-generation multifunctional energy storage electrodes by highlighting the importance of interfacial nanoengineering.

Results & Discussion

Fabrication of Structural Supercapacitor.

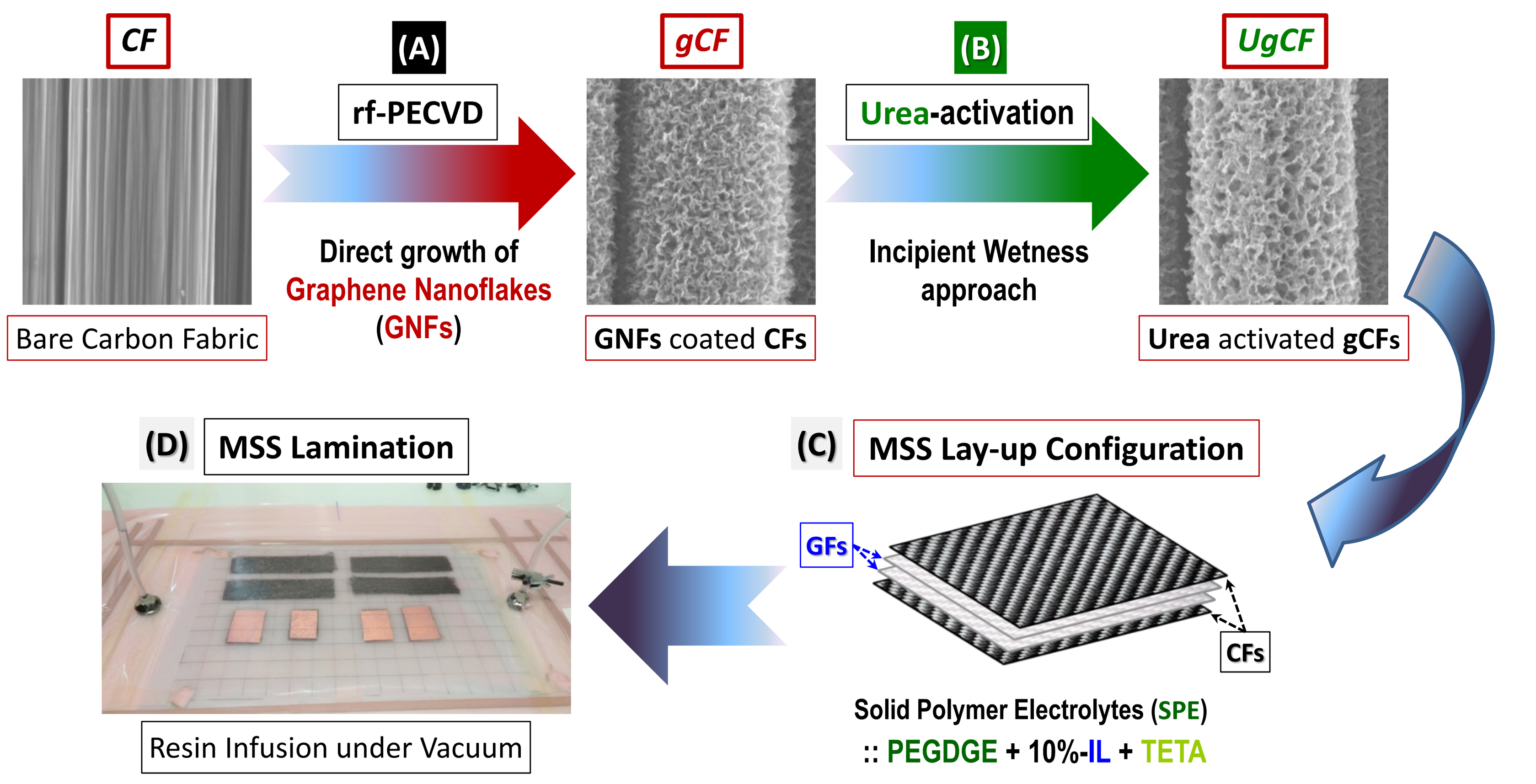

Figure 1: Schematic illustration of steps used for the fabrication of structural supercapacitor: (A) ***CF*** → ***gCF***: Direct growth of graphene nanoflakes (GNFs) on bare carbon fibre (***CF***) fabrics by rf-PECVD. (B) ***gCF*** → ***UgCF***: Urea activation of GNFs-coated carbon fibre (***gCF***) fabrics (***UgCF***). (C) CF-(2GFs:SPE)-CF lay-up configuration of multifunctional structural supercapacitor (MSS). (D) Fabrication of carbon fibre reinforced polymer (CFRP) composites based MSS laminates, via resin infusion method.

Morphological study.

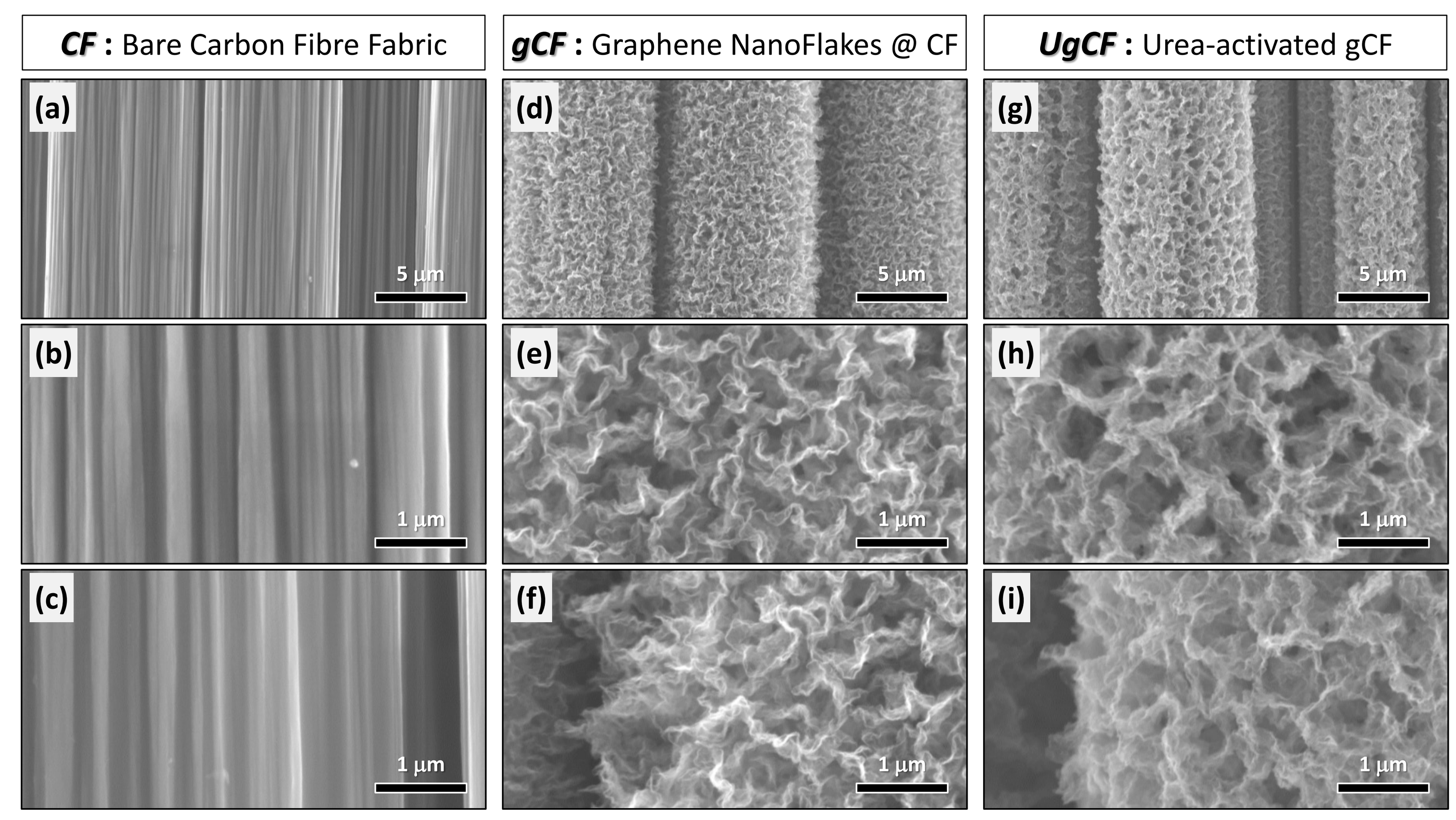

Figure 2: SEM images of different fabrics: (a-c) bare carbon fibre (***CF***); (d-f) Graphene Nanoflakes (GNFs) deposited at carbon fibre (***gCF***); and (g-i) Urea-activated gCF (***UgCF***). The second row (b, e and h) represents images of the top surface of a single fibre, while the corresponding images of the third row (c, f and i) illustrate the sidewall of a single fibre.

Materials characterisations.

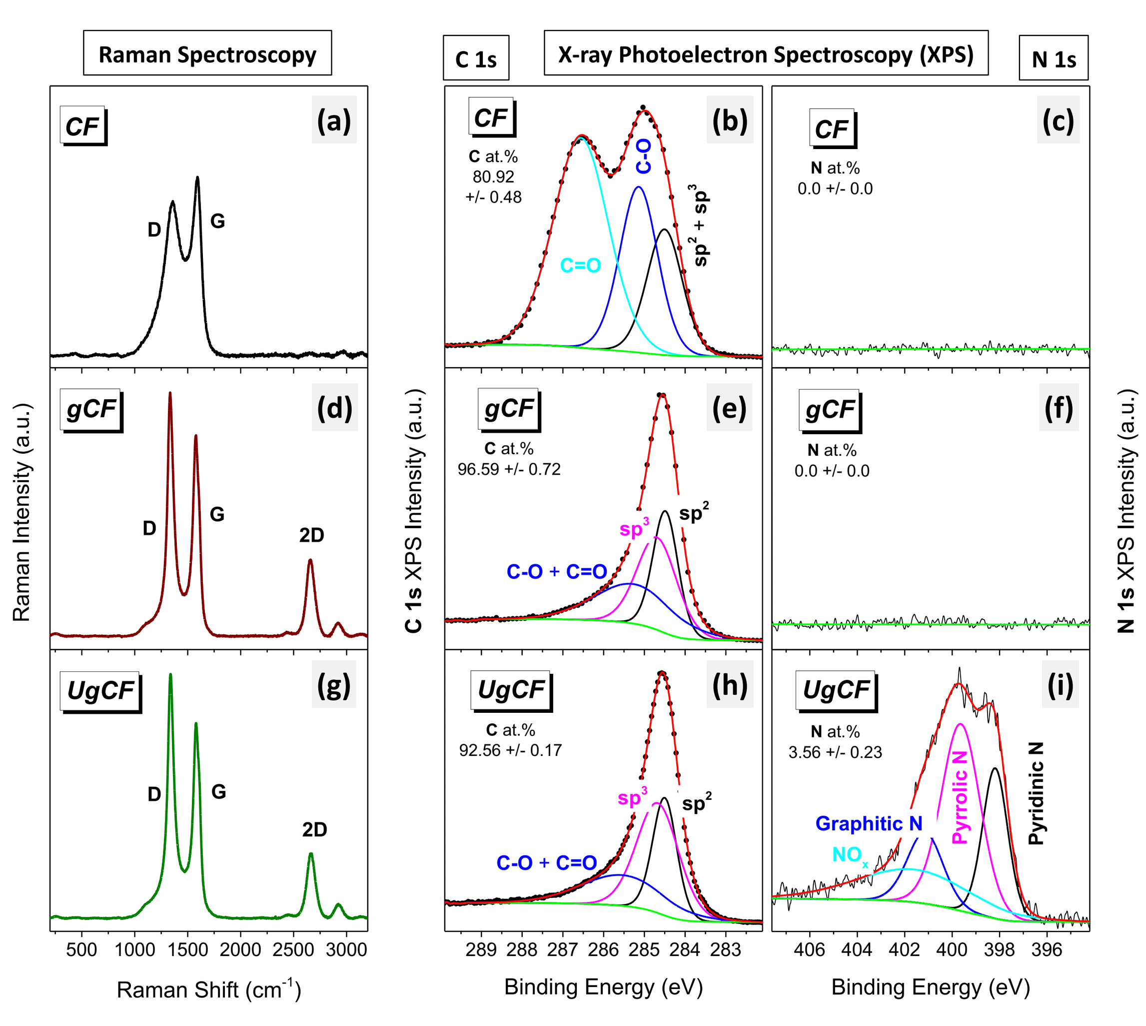

Figure 3: Raman and high-resolution X-ray photoelectron spectroscopic results. Top row: Raman (a) and high-resolution C 1s (b) and N 1s (c) XPS spectra of bare ***CF*** fabrics. Middle row: (d) Raman, (e) C 1s and (f) N 1s spectra of ***gCF*** fabrics. Bottom row: (g) Raman, (h) C 1s and (i) N 1s spectra of ***UgCF*** fabrics.

Electrochemical Performances

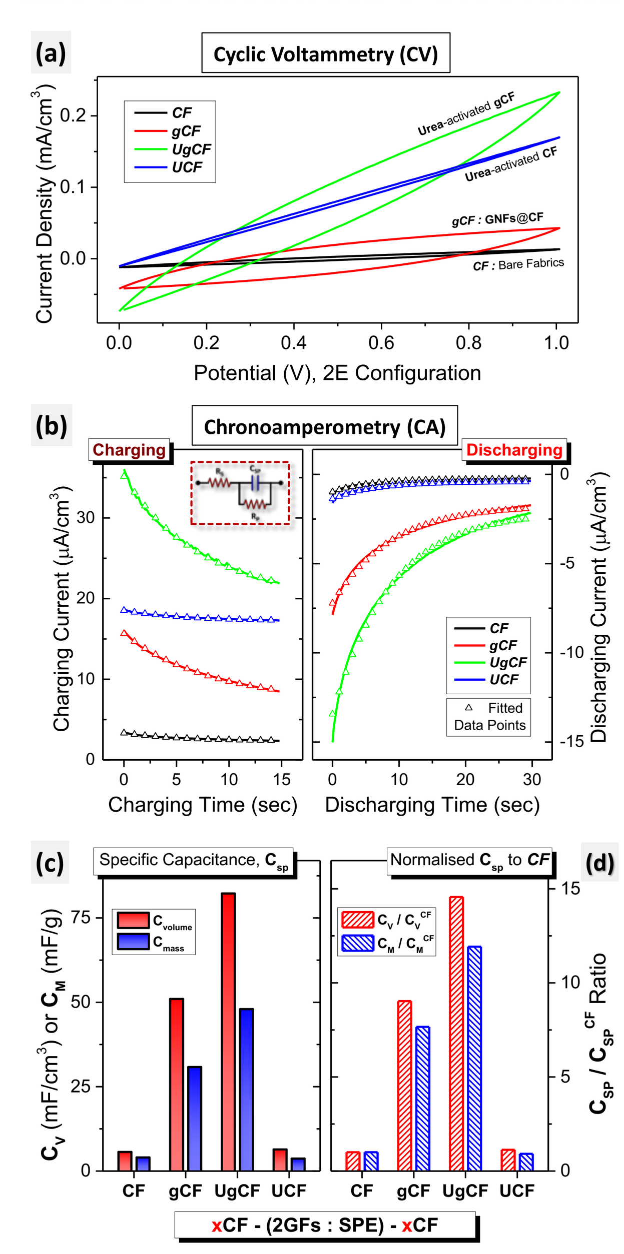

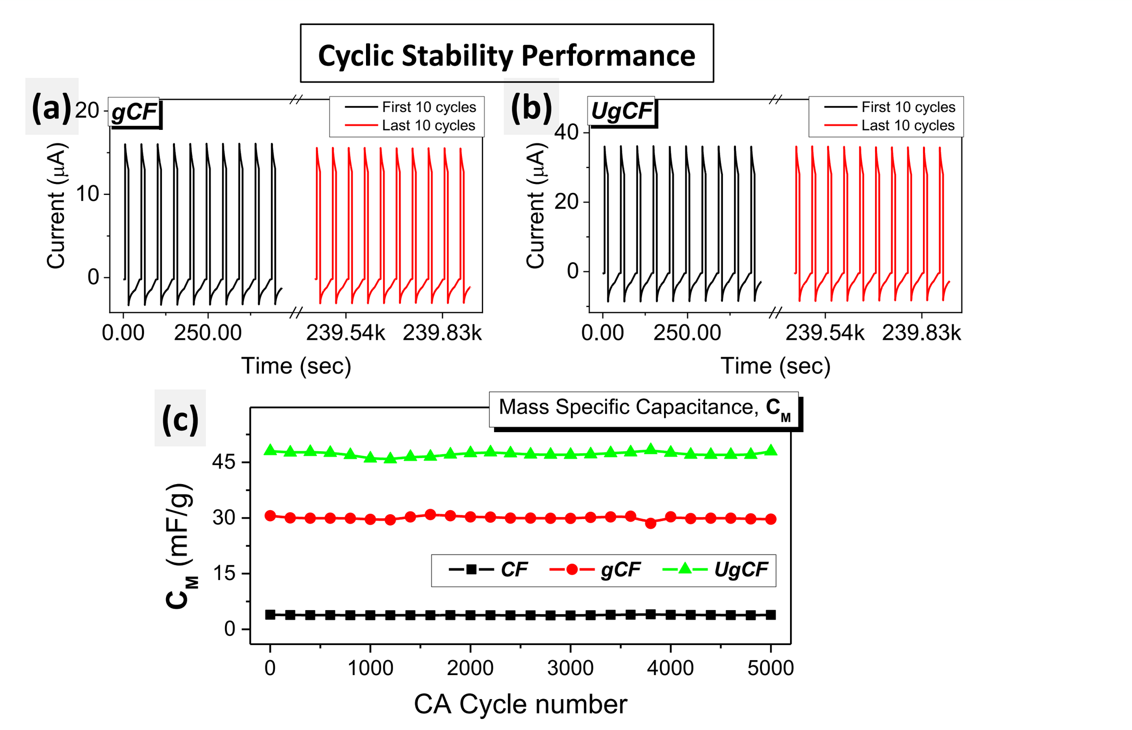

Figure 5: Representative chronoamperometric (CA) plots, for first and last 10 cycles, of total 5000 charge-discharge cycles, recorded in 2-electrode (2E) configuration, for the MSS devices based on (a) gCF and (c) UgCF fabric electrodes. (d) Variation of mass-specific capacitance (C_M) versus number of CA cycles.

Figure 4: (a) Cyclic voltammetry (CV) plots, recorded in 2-electrode (2E) configuration, at a scan rate of 10 mV/s, for the MSS devices based on bare ***CF***, ***gCF***, ***UgCF*** and urea-activated bare CF (***UCF***) fabric electrodes. (b) Respective chronoamperometric (CA) curves, recorded in 2E configuration, applying 0.1 V step potential, representing the charge (left) and discharge (right) performances. The fitted data points were calculated by fitting the CA charge and discharge data to the current transient response of the RC equivalent circuit model (Inset of Figure 4b). (c) Specific capacitance (C_{sp}), derived from Equation S4. (d) Normalized specific capacitance values (C_{sp}/C_{sp}^{CF}) values.

Mechanical performances.

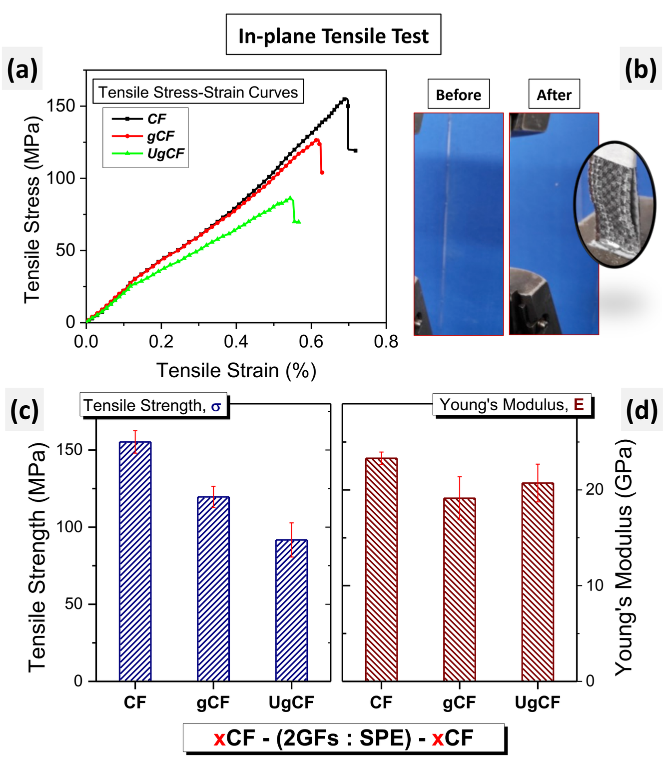

Figure 6: (a) Representative Tensile Stress-Strain curves of various CFRP-laminates, consisting of bare ***CF***, ***gCF*** and ***UgCF***, with CF–(2GFs:SPE)–CF lay-up configuration incorporating two layers of glass fibre (GF) fabric separators. (b) Typical failure of a specimen under tensile test: images collected before (left) and after (right) a typical in-plane tensile test. Right inset displays a typical delamination occurred at the interface between CF electrode and GF separators. (c-d) Comparison of the (c) tensile strength (σ) and (d) Young's modulus (***E***) values of the CFRP-laminates, described above.

Multifunctionality of CFRP-based MSS.

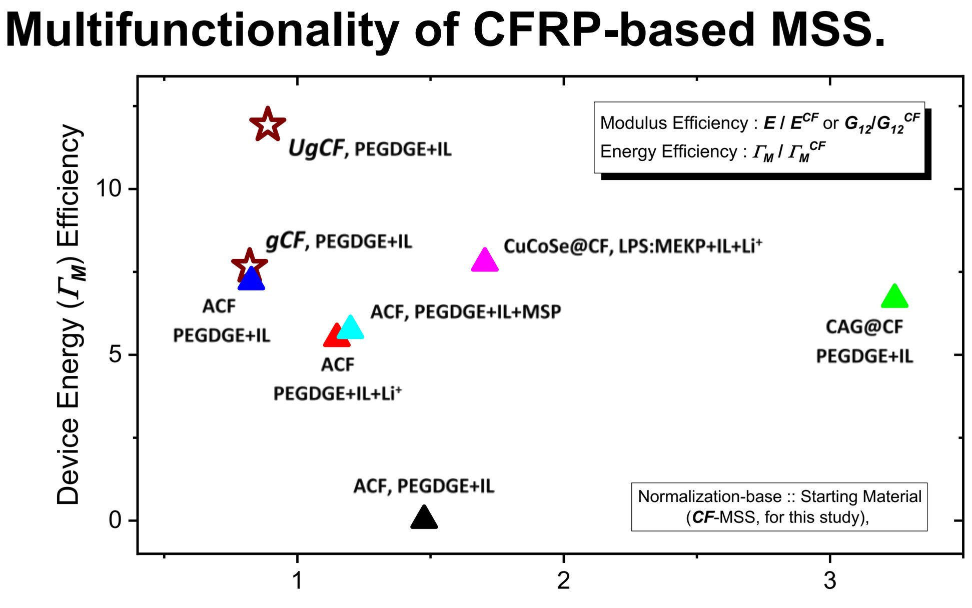

Figure 7: Multifunctional performance, device energy efficiency (normalised energy density, Γ_M/Γ_M^{CF}) versus elastic modulus efficiency (normalised Young's modulus, E/E^{CF} or shear modulus, G_{12}/G_{12}^{CF}) of ***gCF*** and ***UgCF*** based MSS, in comparison to other published MSS systems [6].

Conclusions

- Our study demonstrates the direct growth of GNFs on CF (***gCF***) led to a significant enhancement of C_{sp} by ~9 times and Γ_M by 7.5 times, compared to a conventional bare ***CF*** electrodes based MSS device.
- In advance, the urea activation of GNF-coated fabrics (***UgCF***), which introduced a 3.5 at.% N-doping to the hybrid fabrics, commanded 14- and 12-fold leaps in C_{sp} and Γ_M, relative to control bare CF MSS device.
- Overall, the nitrogen doped GNF-based device offered an improvement in energy efficiency of 12 in terms of Γ_M and a structural efficiency of 0.9 in terms of Young's modulus (***E***), demonstrating a novel and promising approach for improving the "multifunctionality" of the CFRP based MSS.

References & Acknowledgements

1. L. E. Asp and E. S. Greenhalgh. ***Compos. Sci. Technol.***, Vol. **101**, pp 41-61, (**2014**).
2. N. Shirshova, H. Qian, M. S. P. Shaffer, J. H. G. Steinke, E. S. Greenhalgh, P. T. Curtis, A. Kucernak and A. Bismarck. ***Compos. Part A***, Vol. **46**, pp 96-107, (**2013**).
3. H. Qian, A. R. Kucernak, E. S. Greenhalgh, A. Bismarck and M. S. P. Shaffer. ***ACS Appl. Mater. Interfaces***, Vol. **5**, pp 6113-6122, (**2013**).
4. N. G. Shang, P. Papakonstantinou, M. McMullan, M. Chu, A. Stamboulis, A. Potenza, S. S. Dhesi and H. Marchetto. ***Adv. Funct. Mater.***, Vol. **18**, pp 3506-3514, (**2008**).
5. A. Karakassides, A. Ganguly, K. Tsirka, A. S. Paipetis and P. Papakonstantinou. ***ACS Appl. Nano Mater.***, Vol. **3**, pp 2402-2413, (**2020**).
6. A. Ganguly, A. Karakassides, J. Benson, S. Hussain and P. Papakonstantinou. ***ACS Appl. Energy Mater.***, Vol. **3**, pp 4245-4254, (**2020**).

The authors acknowledge the support from the Air Force Office of Scientific Research (**AFOSR**) *under the grant* FA9550-17-1-0042.